Chaperone-bound clients: The importance of being dynamic

Sebastian Hiller[1,*]

[1]Biozentrum, Klingelbergstr. 70, 4056 Basel

*corresponding author: sebastian.hiller@unibas.ch

Abstract

Several recent atomic resolution studies have resolved how chaperones interact with their client proteins. In some cases, molecular chaperones recognize and bind their clients in conformational ensembles that are locally highly dynamic and interconvert, while in other cases, clients bind in unique conformations. The presence of a locally dynamic client ensemble state has important consequences, both for the interpretation of experimental data, and for the functionality of chaperones, as local dynamics facilitate rapid client release, folding on and from the chaperone surface, and client recognition without shape complementarity. Facilitated by the local dynamics, at least some chaperones appear to specifically recognize energetically frustrated sites of partially folded client proteins, such that the release of frustration contributes to the interaction affinity.

Chaperones and their Clientomes

Cells in all kingdoms of life rely on a robustly functioning proteome, both in cellular ground states and under all kinds of different conditions. To ensure that all proteins obtain their correct fold and functionalities at the right time and at the right localization, cells use intricate molecular chaperone systems (1-4). The action of these chaperone systems is crucial for client protein folding, translocation and unfolding. Breakdown of the chaperone system can lead to protein misfolding and aggregation, which then can ultimately cause cell death, neurodegeneration, and other protein misfolding diseases (5, 6). In a typical cell, different types and isoforms of chaperones are organized towards a large functional chaperone network, in which multiple ATP-dependent and ATP-independent chaperones with partially overlapping clientomes act together to protect clients from their conformational progression on non-productive folding pathways (7-11).

A common elementary function shared by many, if not all, soluble molecular chaperones in at least some of their conformational states, is the ability to bind unfolded and partially folded client proteins. This function can be referred to as the holdase function and permits chaperones to interact with client polypeptides for lifetimes that are sufficiently long to exert the biological function of the chaperone. While the holdase function per se is ATP-independent, it is combined in some chaperones with an ATP hydrolysis reaction or other functional regulations towards more complicated functional cycles (12-14). A chaperone that possesses only the holdase function is commonly referred to as a holdase chaperone, while the more complicated functional cycles can give rise to resulting foldase / unfoldase / disaggregase activities.

Structural and functional descriptions of chaperone–client interactions at the atomic level are essential to fully understand a chaperone, as they allow rationalizing the client recognition and client interaction mode, resolve differential interaction between various clients, and the biophysical limitations of the interaction. Crystal structures of the apo (client-free) forms of many molecular chaperones have long been available (15-23), but high-resolution structural descriptions of chaperones in complex with their clients have only recently become available. In particular, the availability of modern high-resolution NMR spectroscopy methods has played an essential role, and most high-resolution structures of protein–client complexes stem from this method. In this review, we aim at discussing the recent structural studies of

chaperone–client complexes and the conclusions that could be drawn on the underlying chaperone–client interaction biophysics.

Atomic resolution structural studies of chaperone–client complexes

The first chaperone–client system with two full-length natural proteins, of which conformation and dynamics could be completely resolved at the atomic level has been the Skp–Omp system (24). The chaperone in this system, bacterial Skp, binds an unfolded outer membrane protein during the diffusive transport across the aqueous periplasm (25, 26). The atomic level data revealed that the client is in constant conformational reorientation and that all local contacts are short-lived, non-specific and transient, while the global contact is long-lived (Figure 1A).

A subsequent study resolved the structural determinants of the bacterial trigger factor (TF) binding the model client protein PhoA (27). In this atomic resolution structure, the client protein was found to bind to the chaperone in a unique conformation (Figure 1B). The population of this lowest energy state of the chaperone–client complex has a population level of 70% or above (27). Notably, the two systems Skp–Omp and TF–PhoA feature two very different binding modes of chaperone–client interaction. While the Skp binds its clients in the form of conformational ensembles, the chaperone TF binds its client PhoA in single dominant conformations for those segments of the client that are in contact with the chaperone. This is well visualized by the sequence coherence of the individual PhoA segments on the chaperone surface (Figure 1B).

A third key study of a chaperone–client complex described the interaction of the chaperone Hsp90 binding a physiological client, the protein Tau that is in turn involved in neurodegenerative diseases (28). This structural description highlighted the presence of a conformational ensemble. The interaction surface of Tau on Hsp90 was mapped to two domains of Hsp90, the N- and the M-domain. Interestingly, these two interaction sites are about ~100 Å apart, thus comprising an extended overall interaction surface. Combination of data from solution NMR spectroscopy and small angle X-ray scattering (SAXS) enabled the derivation of a structural model of the Hsp90–Tau complex, where the Tau ensemble converged strongly on the two binding sites (Figure 1C). Just as for the Skp–Omp complex, this model underscores the importance of multiple non-specific low-affinity contacts to build up towards a global high affinity interaction by avidity (28).

Finally, a fourth study determined the structure of the chaperone-client complex SecB–PhoA at atomic resolution description (29). The structure shows that PhoA is wrapped around SecB in an extended arrangement, and utilizes several SecB client-interaction sites determined by mapping of specific peptides (Figure 1D). The data also allowed to identify that the groove on the SecB surface formed by helices 1 and 2 is able to adjust its size by swinging out helix 2 by up to 50° in order to accommodate large hydrophobic side chains of the client protein. Just as for TF–PhoA, there is a unique arrangement of the interacting segments on the chaperone for SecB–PhoA.

Besides these structure determinations, multiple further studies contributed substantially to resolving atomic details of chaperone-client systems. Some important examples in which solution NMR spectroscopy was used as the main study method are functional studies of the TRiC/CCT system (30), Hsp70 (31-34), GroEL (35, 36), Hsp90 (37, 38) as well as the bacterial ATP-independent holdase chaperone Spy (39, 40). These studies have greatly expanded the current understanding of the biophysical basis of chaperone–client interactions and highlight the power of solution NMR spectroscopy for the study of these dynamics systems. Notably, at the same time, many of the studies remain descriptive in the sense that they do not provide causal biophysical rationales for the chaperone functions. A number of exciting discoveries are thus yet to be expected.

Chaperone–client interaction modes

From the available high-resolution structural studies, the conclusion emerges that chaperone–client complexes come in different types with fundamentally different interaction biophysics. The underlying interaction energy landscapes can be described by two parameters, the entropy of the bound state and the enthalpy difference between the bound and the apo state (41, 42). These parameters define the depth and the width of the interaction landscape, respectively (Figure 2). The enthalpy difference to the apo form, ΔH, is comprised by the enthalpic changes in inter- and intramolecular interactions upon binding. The entropy of the bound state, S^{bound}, quantifies the conformational space that the chaperone–client complex populates. With this parametrization, two limiting cases for the binding mode exist and a given interaction can usually be classified into one of these two cases (Figure 2).

In the “single conformational limit”, the client is bound to the chaperone in a predominant single backbone configuration, with only a small conformational entropy S^{bound} that mainly arises from side chain rotations and other small local rearrangements. The interaction energy landscape is a narrow and deep valley, corresponding in its biophysical properties to classical protein–protein interactions.

In the “multi-conformational complex” (or “fuzzy complex”), in contrast, the client is bound in a multi-conformational ensemble state with large S^{bound}. The large entropy of this ensemble arises mainly from the vast conformational space of the client backbone and consequently, the interaction energy landscape is a broad valley (Figure 2). The ensemble of client structures interconvert in thermal equilibrium while the client remains bound to the chaperone.

For either interaction type, the global affinity is given by the interaction Gibbs free energy, which combines the enthalpic and the entropic contributions relative to the free state.

$$\Delta G = G^{bound} - G^{free} = \Delta H - T(S^{bound} - S^{free})$$

Here, large negative values for ΔG correspond to a high affinity and such large affinities can result from either a large negative ΔH or a large value of S^{bound}. Both interaction types can thus result in high-affinity complexes, however in different ways. The single conformational mode requires a large (negative) enthalpy term ΔH to achieve high affinity, while for the multi-conformational complex the enthalpy term can be considerably lower, because the entropy decrease upon binding of the apo client, $S^{bound} - S^{free}$, is much lower.

At the same time, the enthalpy difference upon binding, ΔH, is related to the specificity of the interaction. A large interaction enthalpy requires a coordinated spatial arrangement of multiple intermolecular interactions, including hydrophobic, polar and electrostatic contacts. Large (negative) ΔH values arising from multiple well-oriented contacts are readily possible in the narrow conformational valley of the single conformational limit, where the chaperone recognizes certain specific segments of the client and binds them in a unique conformation. For the broad interaction landscape of the multi-conformational complex, however, a spatial coordination of multiple favourable local contacts is not occurring. The individual contacts are short-lived and fluctuate between favourable and non-favorable orientations, resulting in a lower ΔH and at the same time in lower requirements for the chemical composition of the

client, i.e. a lower client specificity. In this way, the two different types of interaction mode can relate to a different client specificity of the chaperone.

Technical aspects in describing chaperone-client complexes

In addition to the impact on client specificity, the two interaction modes also lead to fundamentally different regimes for their experimental characterization, in particular for the structure determination of the chaperone–client complexes. An experimental observable *A* obtained from an ensemble will be averaged over the individual subpopulations of the ensemble, up to the time resolution of the particular experimental method. If the kinetic barriers between the individual substates of the bound state are small, a complete averaging of all substates occurs and the observable *A* is an ensemble average.

$$\langle A \rangle = \sum_i p_i A_i \qquad (3)$$

, where *i* is the index of the state, p_i is the population of the state and A_i is the observable in state *i*. If the bound state includes kinetic barriers that are higher than the time resolution of the method, time-averaging is not complete and the bound state splits into several substates, for each of which eq. (3) applies separately. The interpretation of the ensemble-averaged value <*A*> towards a structural model of the ensemble is non-trivial. Only if a single conformer is predominant, i.e. with a single p_1 larger than a certain threshold X, the interpretation protocols of traditional structural biology methods towards a single structure is warranted. Here, X is a relatively large fraction, such as for example 70%, depending on the details of the experimental method.

This situation is briefly exemplified on the example of the intermolecular Nuclear Overhauser effect (NOE), which lies at the heart of conventional protocols for solution NMR structure determinations of rigid proteins and rigid protein-protein complexes (43). The NOE arises from cross-relaxation events of nuclear spins. For a pair of protons $^1H^{(j)}$–$^1H^{(k)}$, with one proton *j* on the chaperone and one proton *k* on the client, the cross-relaxation rate constant in a given protein conformation *i* is given by $\sigma^{jk,i}$, (Figure 3). Because σ is proportional to the inverse sixth power of the interspin distance *r*, for single conformations the NOE can be used to measure spin–spin distances. In conformational ensembles, however, the observed constant σ^{jk} is ensemble-averaged from the individual substates as $\sigma^{jk} = \sum_i p_i \sigma^{jk,i}$ (Figure 3). The extraction of a single distance from this average is no longer possible. While the

application in classical structure determination protocols is prohibitive, the determined value can be used to map chaperone–client interfaces at the atomic level, in particular in situations where the dynamic ensemble features a narrow chemical shift dispersion and the observed cross-peaks in 3D NOESY spectra are a superimposition of multiple substrate spins with similar chemical shifts (44).

As an alternative to the NOE, the use of intermolecular paramagnetic relaxation enhancements (PREs) has been proven worthwhile to derive spatial proximity measurements in the case of conformational ensembles. Just like the NOE, the PRE effects are also ensemble-averaged, but can be used to determine spatial probabilities in first order approximation (24, 45-48). An alternative experimental technique with effects in the distance range of PREs is the pseudo-contact shifts (PCS) . Notably, while PCS are very valuable to obtain distance constraints for static protein–protein complexes, they will presumably be less useful in highly dynamic chaperone–client systems, because the PCS averages towards zero, if the nuclear spin moves between the different space zones of positive and negative PCS contributions. The PRE, in contrast, is of uniform sign (but not magnitude) in all areas of space and will therefore also in a dynamic ensemble add up in a distance-weighted manner .

For X-ray crystallography, the presence of a dynamic ensemble in chaperone–client complexes is typically prohibitive in a fundamental sense, because crystals of the complexes cannot be obtained. Therefore, crystallography studies of chaperone–client complexes were so far successful only in cases, where clients bound in a single conformation, which is particularly possible for short peptides (49-52). With the advent of direct electron detectors, chaperone-client systems have also been studied by cryo-electron microscopy. Beautiful work has outlined conformational changes in chaperone domain dynamics and revealed insight on the client interaction (53-67). It will be interesting to see, if and how future methodological improvements may resolve the client conformational ensemble at the atomic level. Another very powerful method to describe chaperone domain dynamics is single-molecule Förster resonance energy transfer (FRET). This method is able to determine the ensemble statistic of the spatial distances between specifically introduced dye pairs, and thus provides quantitative descriptions of the population and interconversion dynamics of individual conformer states. In the past few years, substantial insights into chaperone dynamics have been obtained with single-molecule FRET . It will be interesting to see, if and how future

methodological improvements may resolve client conformational ensembles and chaperone–client interactions at the atomic level.

Functional impact of the dynamics

In addition to the impact on specificity and on the choice of experimental methods, the presence of ensemble dynamics of the client on the chaperone surface has two significant functional consequences. Firstly, in the single conformational limit, the local and the global dissociation rate constants are essentially identical. In contrast, the multi-conformational complex allows for a substantial difference in these two properties, as the client can reform its conformation without leaving the chaperone. The local correlation lifetime and the global complex lifetime can thus differ by up to at least six orders of magnitude (24). This time difference allows for fast, energy-independent client release kinetics, because the client release to a downstream target or receptor is limited by the local, not the global contact time (68). Such functionality is for example relevant for membrane protein holdases, which require long lifetimes to avoid aggregation during transport, but nonetheless fast, ATP-independent client release (68). Secondly, the dynamic conformational reorientation on the chaperone surface allows for folding of the protein while bound to the chaperone surface. The existence of this property had initially been discovered for GroEL and has recently also been described for the Spy–Im7 system, where the client folds while bound to the chaperone (69, 70).

A combination of the two effects has been observed in the case of a membrane protein client bound to the periplasmic chaperones Skp and SurA. Single-molecule force spectroscopy and NMR spectroscopy could show that a model client protein, the large β-barrel outer membrane receptor FhuA from *Escherichia coli* is stabilized in a dynamic, unfolded state on the chaperone surface, which prevented it from misfolding (Figure 4) (68). The dynamics of the bound state allows the client protein to explore local structural configurations, such that the SurA-chaperoned FhuA polypeptide stepwise inserts β-hairpins into the membrane until the entire barrel is folded. The membrane thus acts as a free energy sink for hairpin insertion and physically separates transiently folded structures from the chaperone, funnelling the FhuA polypeptide towards its native conformation. Notably, while the lifetime of the chaperone–client complex is in the minutes to hours range, folding from the chaperone into

the membrane occurs on the seconds timescale, constituting fast release in an ATP-independent manner (68).

Dynamic recognition of frustrated sites on native client proteins

In the case of native, i.e. folded or partially folded protein clients, the presence of non-specific, highly dynamic conformational interaction modes allows for two relevant functional features. Firstly, the multi-conformational complexes not only enable promiscuity, but also ease the constraints from potential steric overlap between the interaction surfaces, because the dynamic interactions of chaperones with native client proteins do not require structural shape complementarity, providing a further rationale for chaperone promiscuousness and the generally observed broad clientomes (71).

Secondly, the conformational interconversions allow for a mode of client recognition in that chaperones recognize and bind the locally frustrated sites on the client proteins. Local frustration in biomolecules can exist between chemical groups of the polypeptide chain, when they are forced into energetically unfavourable contacts by other, well-folded parts of the protein such that no energetically favourable local rearrangement is possible (72-75). The occurrence of frustration is a fundamental concept in molecular biology and among others a driving force underlying protein folding . Notably, the presence of frustration is frequently correlated to local instability of proteins, since unfavourable contacts between individual pairs of amino acid side chains at frustrated sites induce dynamic rearrangements and thus instability . Several holdase chaperones now appear to interact with locally frustrated areas of partially folded client proteins by stabilizing conformations that are unfavorable in the absence of the chaperone (40, 71). This release of local frustration contributes to the interaction affinity and provides a local recognition motif that is sequence-unspecific. The presence of such an interaction mechanism has been shown so far for three different chaperones – the periplasmic Spy, SurA and Skp – and two different clients, the partially folded model client proteins SH3 and Im7, as well as for the dimeric form of the chaperone TF (Figure 5) (40, 71, 76). These observations imply that the principle of recognizing frustrated segments in native clients could be of a more general nature, making further studies in this direction highly interesting.

Concluding Remarks and Future Perspective

Taken together, the recent years have brought unique insights into conformations and dynamics of chaperone–client systems at the atomic level, with a strong contribution from solution NMR spectroscopy. Additional advances will likely come from integrative structural biology approaches that combine data from several complementary techniques to overcome the limitations of the individual approaches. In fact, most of the studies discussed in this review are already based on an integrative approach, such as by interpreting dynamics data from NMR or FRET on the basis of previously determined crystal structures of the chaperone apo forms. Nonetheless, the field is not yet in a position to infer the functional mechanisms of chaperones from knowledge of their apo structures alone and key questions remain to be answered in the coming years (see outstanding questions box). Further detailed studies of chaperone systems at the atomic level are required to fully explore the space of chaperone–client interactions. This knowledge gap includes not only soluble chaperones but in particular also membrane-standing insertase chaperones (77-82), since no structural information on their client insertion processes are available at the atomic level. In addition, new methodological developments that quantify dynamic multi-conformational complexes better than existing technology are highly desired.

Acknowledgements

Research funding by the Swiss National Science Foundation is gratefully acknowledged.

Figures

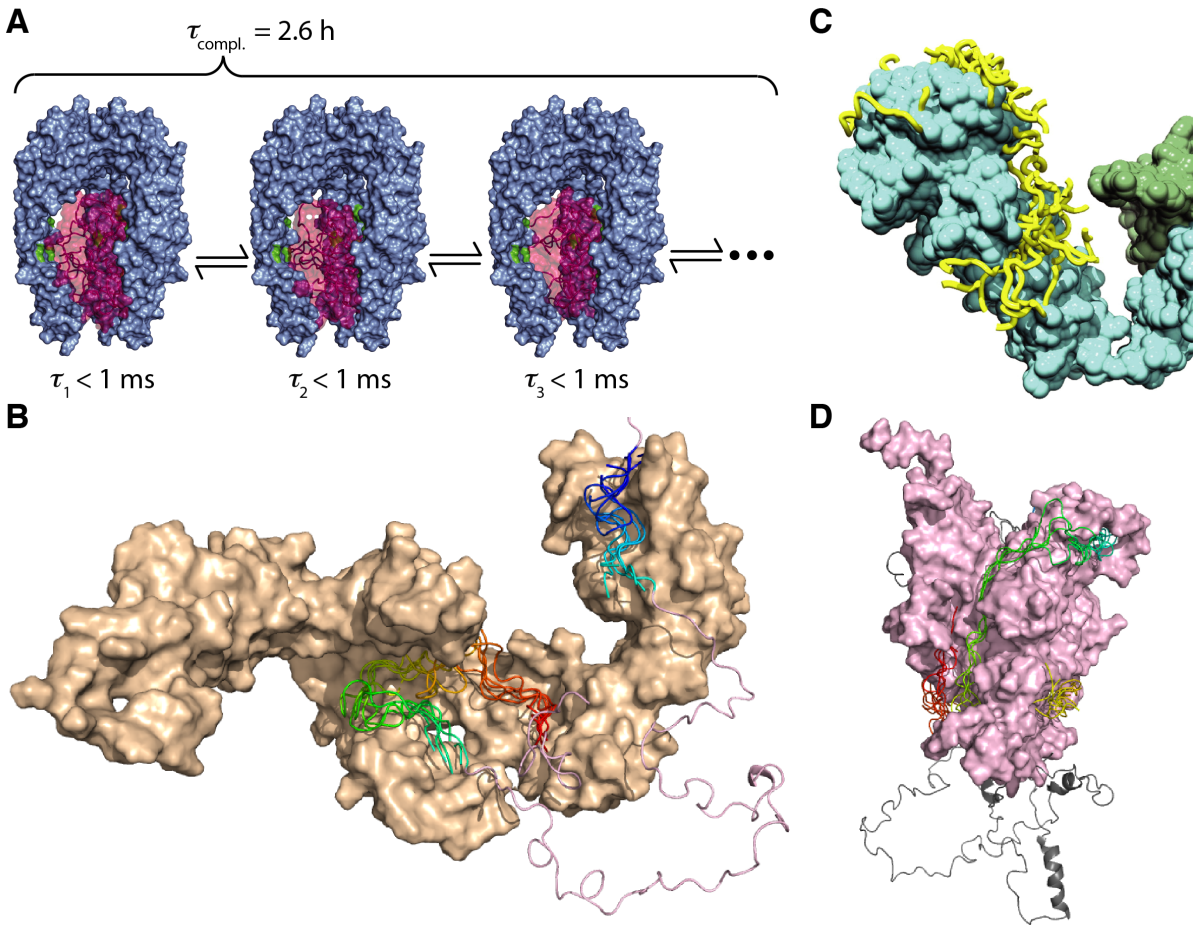

Figure 1. Gallery of selected chaperone–client complexes. (A) The conformational equilibrium of the Skp–OmpX complex (blue-purple) is an ensemble of interconverting conformations in fast equilibrium with a global lifetime of $\tau_{compl.}$ of 2.6 h. Individual conformations *i* have lifetimes τ_i < 1 ms (24). (B) Solution NMR structure of TF in complex with the polypeptide segment PhoA (1–150) (PDB 2MLY) (27). TF is shown as a solvent-exposed surface in beige and one PhoA conformer as a pink ribbon. For four additional conformers of PhoA, only the segments binding to TF are shown. These are rainbow-colored from N- to C-terminus, highlighting their sequence coherence on the TF surface. (C) Convergence of Tau models on Hsp90 based on NMR and SAXS data (28). The ten best Tau models bound to Hsp90 (Tau models, yellow bands; Tau-binding Hsp90 protomer, cyan; other Hsp90 protomer, green). Reproduced with permission from (28). (D) Solution NMR structure of the SecB−PhoA complex (PDB 5JTL) (29). SecB is shown as a space-filling model in pink. Color code for five PhoA conformers as in panel B.

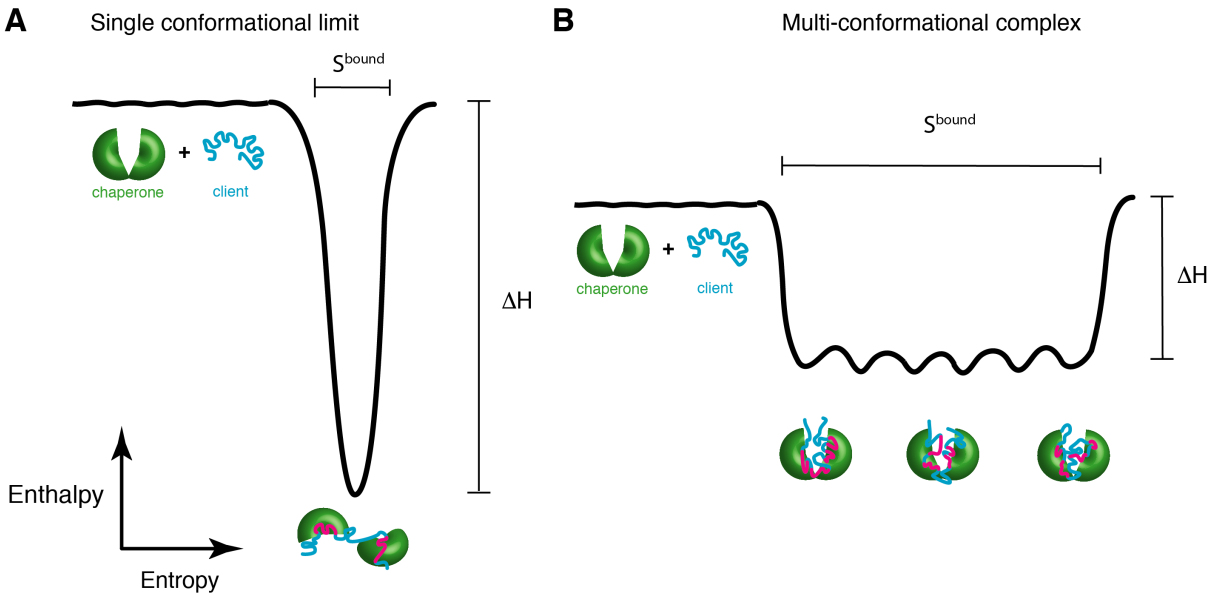

Figure 2. The two primary modes of chaperone–client interaction. (A) Interaction energy landscape of the "single conformational limit". The client (blue) binds to the chaperone (green) at well-defined interaction sites (magenta). The chaperone-bound segments (magenta) adopt a well-defined structure. (B) Interaction energy landscape of the "multi-conformational complex". The client binds to the chaperone as an interchanging conformational ensemble. Segments of the client that are interacting with the chaperone at one time point change their structure and interaction with the chaperone at other time points. The enthalpy differences between the client apo and holo form, ΔH, and the entropy of the bound state, S^{bound} is indicated. Adapted from (83).

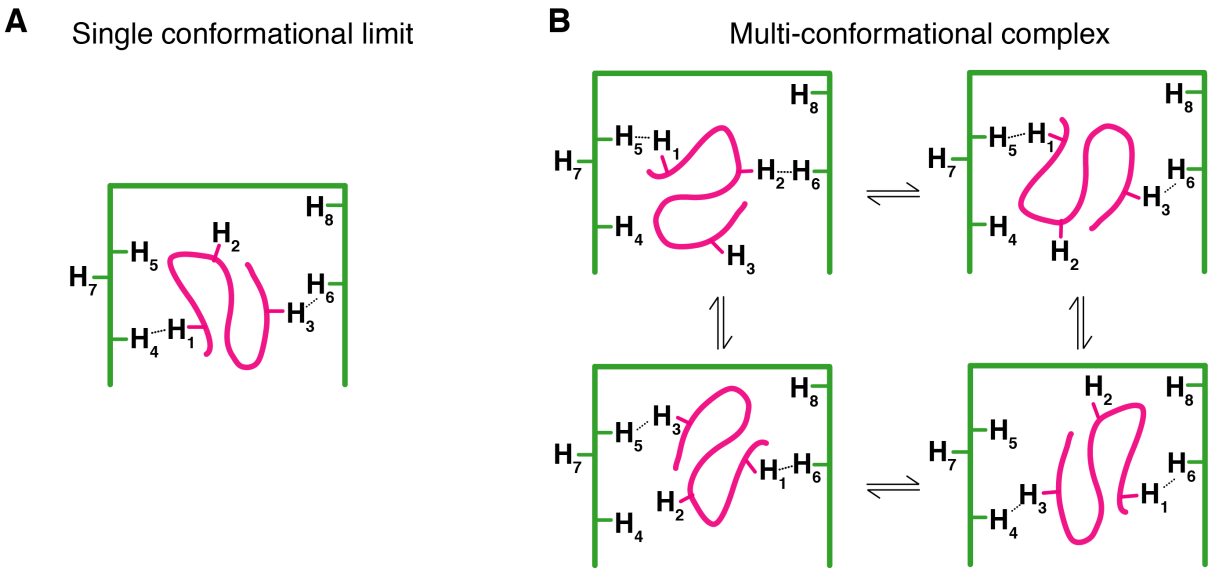

Figure 3. Signal averaging in conformational ensembles on the example of the intermolecular NOEs. Schematic model of conformations of unfolded client (purple) in complex with a molecular chaperone (green) in (A) the single conformational limit and (B) the multi-conformational complex. Eight protons H_1–H_8 are highlighted. For each client conformation, pairs of protons involved in short-range contacts, corresponding to strong intermolecular NOEs, are connected with dashed lines. The total NOE signal results from an ensemble average as described by eq. (3). Therefore the NOE data in A contain the information to calculate the underlying single conformation, while the NOE data in B are not all fulfilled by a single structure. Adapted from (44).

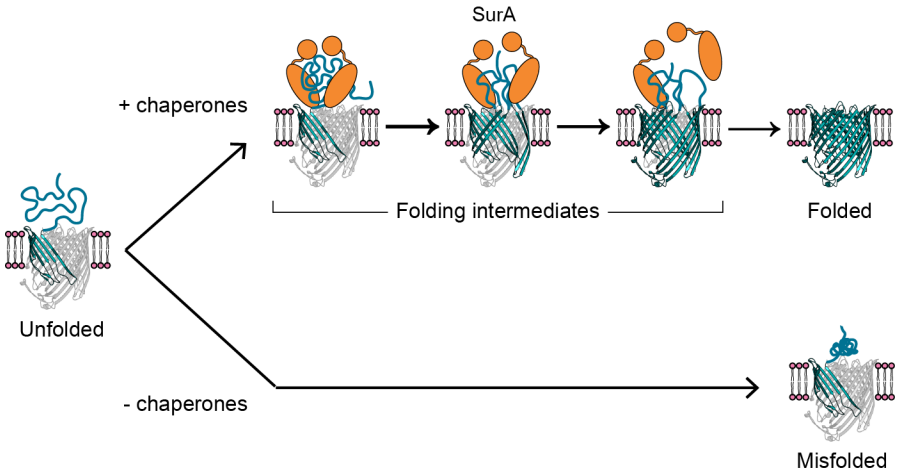

Figure 4. Folding pathways of the chaperone-bound membrane protein FhuA into the membrane. Insertion and folding pathways of FhuA in the absence of chaperones and in the presence of SurA (orange). Without chaperones the majority of unfolded FhuA receptors misfold (bottom). The misfolded polypeptide is assumed to locate inside and/or outside the membrane. Presence of SurA stabilizes the unfolded state of FhuA and promotes stepwise insertion and folding of β-hairpins into the lipid membrane. This stepwise insertion of secondary structures proceeds until the substrate has completed the folding of the receptor. Adapted from (68).

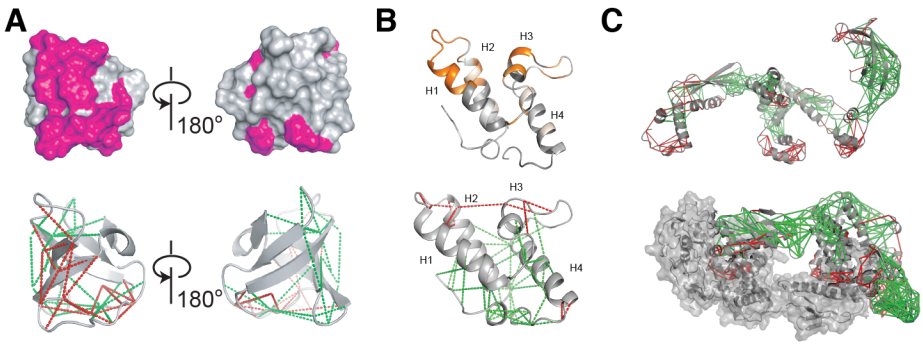

Figure 5. Recognition of frustrated sites by molecular chaperones. (A) Top: Interaction surface of the chaperone Spy (magenta), on the crystal structure of the client SH3 (PDB 3UA6). Bottom: Local frustration of SH3. (B) Top: Interaction site of the chaperone Spy (orange) on the client protein Im7 (PDB 1AYI). Bottom: Local frustration of Im7. (C) Structural frustration of the monomer (PDB 1W26) and the dimer of the chaperone trigger factor (76). In all panels, local frustration was calculated with the software Frustratometer (75). Minimally frustrated interactions are depicted as green lines, highly frustrated interactions as red lines. Reprinted from (40, 71, 76) with permission.

Abbreviation list for Figure captions

TF	trigger factor
OmpX	Outer membrane protein X
Skp	Chaperone seventeen kilodalton protein
NMR	Nuclear magnetic resonance
PhoA	Alkaline phosphatase
PDB	Protein data bank
SAXS	Small-angle X-ray scattering
SecB	Secretion protein B
NOE	Nuclear Overhauser effect
FhuA	Ferric hydroxamate uptake protein A
SurA	Survival factor A
Spy	Chaperone Spy
SH3	SRC homology 3 domain
Im7	Colicin-E7 immunity protein

References

1. Hartl, F.U. *et al.* (2011) Molecular chaperones in protein folding and proteostasis. *Nature* 475, 324-332
2. Bukau, B. *et al.* (2006) Molecular chaperones and protein quality control. *Cell* 125, 443-451
3. Georgescauld, F. *et al.* (2014) GroEL/ES Chaperonin Modulates the Mechanism and Accelerates the Rate of TIM-Barrel Domain Folding. *Cell* 157, 922-934
4. Schopf, F.H. *et al.* (2017) The HSP90 chaperone machinery. *Nat Rev Mol Cell Biol* 18, 345-360
5. Hartl, F.U. (2017) Protein Misfolding Diseases. *Annu Rev Biochem* 86, 21-26
6. Klaips, C.L. *et al.* (2018) Pathways of cellular proteostasis in aging and disease. *J Cell Biol* 217, 51-63
7. Wruck, F. *et al.* (2018) Protein Folding Mediated by Trigger Factor and Hsp70: New Insights from Single-Molecule Approaches. *J Mol Biol* 430, 438-449
8. Sontag, E.M. *et al.* (2017) Mechanisms and Functions of Spatial Protein Quality Control. *Annu Rev Biochem* 86, 97-122
9. Barducci, A. and De Los Rios, P. (2015) Non-equilibrium conformational dynamics in the function of molecular chaperones. *Curr Opin Struct Biol* 30, 161-169
10. Schlecht, R. *et al.* (2011) Mechanics of Hsp70 chaperones enables differential interaction with client proteins. *Nat Struct Mol Biol* 18, 345-351
11. Horwich, A.L. and Fenton, W.A. (2009) Chaperonin-mediated protein folding: using a central cavity to kinetically assist polypeptide chain folding. *Q Rev Biophys* 42, 83-116
12. De Los Rios, P. and Goloubinoff, P. (2016) Hsp70 chaperones use ATP to remodel native protein oligomers and stable aggregates by entropic pulling. *Nat Struct Mol Biol* 23, 766-769
13. Goloubinoff, P. *et al.* (2018) Chaperones convert the energy from ATP into the nonequilibrium stabilization of native proteins. *Nat Chem Biol* 14, 388-395
14. Hartl, F.U. and Hayer-Hartl, M. (2013) The first chaperonin. *Nat Rev Mol Cell Biol* 14, 611
15. Braig, K. *et al.* (1994) The crystal structure of the bacterial chaperonin GroEL at 2.8 A. *Nature* 371, 578-586
16. Kityk, R. *et al.* (2012) Structure and dynamics of the ATP-bound open conformation of Hsp70 chaperones. *Mol Cell* 48, 863-874

17. Ali, M.M. *et al.* (2006) Crystal structure of an Hsp90-nucleotide-p23/Sba1 closed chaperone complex. *Nature* 440, 1013-1017
18. Ferbitz, L. *et al.* (2004) Trigger factor in complex with the ribosome forms a molecular cradle for nascent proteins. *Nature* 431, 590-596
19. Webb, C.T. *et al.* (2006) Crystal structure of the mitochondrial chaperone TIM9.10 reveals a six-bladed alpha-propeller. *Mol Cell* 21, 123-133
20. Walton, T.A. and Sousa, M.C. (2004) Crystal structure of Skp, a prefoldin-like chaperone that protects soluble and membrane proteins from aggregation. *Mol Cell* 15, 367-374
21. Korndörfer, I.P. *et al.* (2004) Structure of the periplasmic chaperone Skp suggests functional similarity with cytosolic chaperones despite differing architecture. *Nat Struct Mol Biol* 11, 1015-1020
22. Bitto, E. and McKay, D.B. (2002) Crystallographic structure of SurA, a molecular chaperone that facilitates folding of outer membrane porins. *Structure* 10, 1489-1498
23. Xu, Z. *et al.* (2000) Crystal structure of the bacterial protein export chaperone secB. *Nat Struct Biol* 7, 1172-1177
24. Burmann, B.M. *et al.* (2013) Conformation and dynamics of the periplasmic membrane-protein-chaperone complexes OmpX-Skp and tOmpA-Skp. *Nat Struct Mol Biol* 20, 1265-1272
25. Rizzitello, A.E. *et al.* (2001) Genetic evidence for parallel pathways of chaperone activity in the periplasm of Escherichia coli. *J Bacteriol* 183, 6794-6800
26. Schiffrin, B. *et al.* (2016) Skp is a multivalent chaperone of outer-membrane proteins. *Nat Struct Mol Biol* 23, 786-793
27. Saio, T. *et al.* (2014) Structural basis for protein antiaggregation activity of the trigger factor chaperone. *Science* 344, 1250494
28. Karagöz, G.E. *et al.* (2014) Hsp90-tau complex reveals molecular basis for specificity in chaperone action. *Cell* 156, 963-974
29. Huang, C. *et al.* (2016) Structural basis for the antifolding activity of a molecular chaperone. *Nature* 537, 202-206
30. Joachimiak, L.A. *et al.* (2014) The structural basis of substrate recognition by the eukaryotic chaperonin TRiC/CCT. *Cell* 159, 1042-1055
31. Zhuravleva, A. *et al.* (2012) An interdomain energetic tug-of-war creates the allosterically active state in Hsp70 molecular chaperones. *Cell* 151, 1296-1307

32. Libich, D.S. *et al.* (2013) Probing the transient dark state of substrate binding to GroEL by relaxation-based solution NMR. *Proc Natl Acad Sci U S A* 110, 11361-11366

33. Sekhar, A. *et al.* (2015) Mapping the conformation of a client protein through the Hsp70 functional cycle. *Proc Natl Acad Sci U S A* 112, 10395-10400

34. Rosenzweig, R. *et al.* (2013) Unraveling the mechanism of protein disaggregation through a ClpB-DnaK interaction. *Science* 339, 1080-1083

35. Libich, D.S. *et al.* (2017) Confinement and Stabilization of Fyn SH3 Folding Intermediate Mimetics within the Cavity of the Chaperonin GroEL Demonstrated by Relaxation-Based NMR. *Biochemistry* 56, 903-906

36. Libich, D.S. *et al.* (2015) Intrinsic unfoldase/foldase activity of the chaperonin GroEL directly demonstrated using multinuclear relaxation-based NMR. *Proc Natl Acad Sci U S A* 112, 8817-8823

37. Oroz, J. *et al.* (2017) Mechanistic basis for the recognition of a misfolded protein by the molecular chaperone Hsp90. *Nat Struct Mol Biol* 24, 407-413

38. Park, S.J. *et al.* (2011) The client protein p53 adopts a molten globule-like state in the presence of Hsp90. *Nat Struct Mol Biol* 18, 537-541

39. Salmon, L. *et al.* (2016) Capturing a Dynamic Chaperone-Substrate Interaction Using NMR-Informed Molecular Modeling. *J Am Chem Soc* 138, 9826-9839

40. He, L. *et al.* (2016) A molecular mechanism of chaperone-client recognition. *Sci Adv* 2, e1601625

41. Burmann, B.M. and Hiller, S. (2015) Chaperones and chaperone-substrate complexes: Dynamic playgrounds for NMR spectroscopists. *Prog Nucl Magn Reson Spectrosc* 86-87C, 41-64

42. Heller, G.T. *et al.* (2015) Targeting disordered proteins with small molecules using entropy. *Trends Biochem Sci* 40, 491-496

43. Wüthrich, K. (1986) *NMR of Proteins and Nucleic Acids* (Wiley, New York)

44. Callon, M. *et al.* (2014) Structural Mapping of a Chaperone-Substrate Interaction Surface. *Angew Chem Int Ed Engl* 53, 5069-5072

45. Otting, G. (2008) Prospects for lanthanides in structural biology by NMR. *J Biomol NMR* 42, 1-9

46. Gillespie, J.R. and Shortle, D. (1997) Characterization of long-range structure in the denatured state of staphylococcal nuclease. I. Paramagnetic relaxation enhancement by nitroxide spin labels. *J Mol Biol* 268, 158-169

47. Gillespie, J.R. and Shortle, D. (1997) Characterization of long-range structure in the denatured state of staphylococcal nuclease. II. Distance restraints from paramagnetic relaxation and calculation of an ensemble of structures. *J Mol Biol* 268, 170-184

48. Lietzow, M.A. *et al.* (2002) Mapping long-range contacts in a highly unfolded protein. *J Mol Biol* 322, 655-662

49. Scheufler, C. *et al.* (2000) Structure of TPR domain-peptide complexes: critical elements in the assembly of the Hsp70-Hsp90 multichaperone machine. *Cell* 101, 199-210

50. Xu, X. *et al.* (2007) The periplasmic bacterial molecular chaperone SurA adapts its structure to bind peptides in different conformations to assert a sequence preference for aromatic residues. *J Mol Biol* 373, 367-381

51. Chen, L. and Sigler, P.B. (1999) The crystal structure of a GroEL/peptide complex: plasticity as a basis for substrate diversity. *Cell* 99, 757-768

52. Martinez-Hackert, E. and Hendrickson, W.A. (2009) Promiscuous substrate recognition in folding and assembly activities of the trigger factor chaperone. *Cell* 138, 923-934

53. Lavery, L.A. *et al.* (2014) Structural asymmetry in the closed state of mitochondrial Hsp90 (TRAP1) supports a two-step ATP hydrolysis mechanism. *Mol Cell* 53, 330-343

54. Verba, K.A. *et al.* (2016) Atomic structure of Hsp90-Cdc37-Cdk4 reveals that Hsp90 traps and stabilizes an unfolded kinase. *Science* 352, 1542-1547

55. Verba, K.A. and Agard, D.A. (2017) How Hsp90 and Cdc37 Lubricate Kinase Molecular Switches. *Trends Biochem Sci* 42, 799-811

56. Kirschke, E. *et al.* (2014) Glucocorticoid receptor function regulated by coordinated action of the Hsp90 and Hsp70 chaperone cycles. *Cell* 157, 1685-1697

57. Roh, S.H. *et al.* (2017) Subunit conformational variation within individual GroEL oligomers resolved by Cryo-EM. *Proc Natl Acad Sci U S A* 114, 8259-8264

58. Ratzke, C. *et al.* (2014) Four-colour FRET reveals directionality in the Hsp90 multicomponent machinery. *Nat Commun* 5, 4192

59. Jahn, M. *et al.* (2014) The charged linker of the molecular chaperone Hsp90 modulates domain contacts and biological function. *Proc Natl Acad Sci U S A* 111, 17881-17886

60. Baytshtok, V. *et al.* (2015) Assaying the kinetics of protein denaturation catalyzed by AAA+ unfolding machines and proteases. *Proc Natl Acad Sci U S A* 112, 5377-5382
61. Rehn, A. *et al.* (2016) Allosteric Regulation Points Control the Conformational Dynamics of the Molecular Chaperone Hsp90. *J Mol Biol* 428, 4559-4571
62. Hellenkamp, B. *et al.* (2017) Multidomain structure and correlated dynamics determined by self-consistent FRET networks. *Nat Methods* 14, 174-180
63. Avellaneda, M.J. *et al.* (2017) The chaperone toolbox at the single-molecule level: From clamping to confining. *Protein Sci* 26, 1291-1302
64. Yang, J. *et al.* (2017) Conformation transitions of the polypeptide-binding pocket support an active substrate release from Hsp70s. *Nat Commun* 8, 1201
65. Kopp, M.C. *et al.* (2018) In vitro FRET analysis of IRE1 and BiP association and dissociation upon endoplasmic reticulum stress. *Elife* 7
66. Rosam, M. *et al.* (2018) Bap (Sil1) regulates the molecular chaperone BiP by coupling release of nucleotide and substrate. *Nat Struct Mol Biol* 25, 90-100
67. Tsuboyama, K. *et al.* (2018) Conformational Activation of Argonaute by Distinct yet Coordinated Actions of the Hsp70 and Hsp90 Chaperone Systems. *Mol Cell* 70, 722-729.e4
68. Thoma, J. *et al.* (2015) Impact of holdase chaperones Skp and SurA on the folding of β-barrel outer-membrane proteins. *Nat Struct Mol Biol* 22, 795-802
69. Horowitz, S. *et al.* (2017) Folding while bound to chaperones. *Curr Opin Struct Biol* 48, 1-5
70. Stull, F. *et al.* (2016) Substrate protein folds while it is bound to the ATP-independent chaperone Spy. *Nat Struct Mol Biol* 23, 53-58
71. He, L. and Hiller, S. (2018) Common Patterns in Chaperone Interactions with a Native Client Protein. *Angew Chem Int Ed Engl* 57, 5921-5924
72. Ferreiro, D.U. *et al.* (2014) Frustration in biomolecules. *Q Rev Biophys* 47, 285-363
73. Ferreiro, D.U. *et al.* (2018) Frustration, function and folding. *Curr Opin Struct Biol* 48, 68-73
74. Onuchic, J.N. and Wolynes, P.G. (2004) Theory of protein folding. *Curr Opin Struct Biol* 14, 70-75
75. Parra, R.G. *et al.* (2016) Protein Frustratometer 2: a tool to localize energetic frustration in protein molecules, now with electrostatics. *Nucleic Acids Res* 44, W356-W360

76. Morgado, L. *et al.* (2017) The dynamic dimer structure of the chaperone Trigger Factor. *Nat Commun* 8, 1992

77. Jores, T. and Rapaport, D. (2017) Early stages in the biogenesis of eukaryotic β-barrel proteins. *FEBS Lett* 591, 2671-2681

78. Kumazaki, K. *et al.* (2014) Structural basis of Sec-independent membrane protein insertion by YidC. *Nature* 509, 516-520

79. Van den Berg, B. *et al.* (2004) X-ray structure of a protein-conducting channel. *Nature* 427, 36-44

80. Gruss, F. *et al.* (2013) The structural basis of autotransporter translocation by TamA. *Nat Struct Mol Biol* 20, 1318-1320

81. Noinaj, N. *et al.* (2013) Structural insight into the biogenesis of β-barrel membrane proteins. *Nature* 501, 385-390

82. Gu, Y. *et al.* (2016) Structural basis of outer membrane protein insertion by the BAM complex. *Nature* 531, 64-69

83. Hiller, S. and Burmann, B.M. (2018) Chaperone-client complexes: A dynamic liaison. *J Magn Reson* 289, 142-155